J. Chem. Sci. (2019)131:101
https://doi.org/10.1007/s12039-019-1678-6

REGULAR ARTICLE

Cobalt nitride nanoflakes supported on Ni foam as a high-performance bifunctional catalyst for hydrogen production *via* urea electrolysis

YANMIN CHEN[a], PEIJIAN SUN[b,*] and WEIWEI XING[c]
[a]College of Chemistry and Chemical Engineering, Zhengzhou Normal University, No. 6 Yingcai Street, Zhengzhou 450044, China
[b]Zhengzhou Tobacco Research Institute of CNTC, No. 2 Fengyang Street, Zhengzhou 450001, China
[c]Faculty of General Education, Zhengzhou Technology and Business University, No. 8 Qiancheng Road, Zhengzhou 451400, China
E-mail: pjsunztri@163.com

MS received 7 May 2019; revised 8 July 2019; accepted 11 July 2019

Abstract. Substituting low theoretical potential of the urea oxidation reaction (UOR) for the high theoretical potential of water splitting at the anode (oxygen evolution reaction) is meaningful for hydrogen energy storage and conversion. In this work, a bifunctional catalyst, cobalt nitride nanoflakes supported on Ni foam (CoN NF/NF), was synthesized for both UOR and hydrogen evolution reaction (HER). A two-electrode electrolyzer (CoN NF/NF||CoN NF/NF) was constructed. To drive 100 mA/cm^2, the voltage of CoN NF/NF||CoN NF/NF only 1.698 V is required, which is much lower than that of Pt/C||IrO_2 (1.860 V) and the current density can be maintained for 30 h.

Keywords. UOR; bifunctional; catalyst; HER.

1. Introduction

The consumption of fossil fuels has led to an urgent need to develop sustainable clean energy to solve the energy crisis.[1–5] Hydrogen energy as a rich resource, high energy, and green energy of no secondary pollution is considered to be the ideal energy source for replacing fossil energy.[6] Currently, hydrogen evolution reaction (HER) from electrochemical water splitting represents an emerging key technology for long-term storage of electricity from renewable sources to reduce intermittent supply as one of the most efficient methods to produce hydrogen.[7–10] However, oxygen evolution reaction (OER) as the anode of water splitting, has a high theoretical oxidation potential (1.23 V). This will greatly limit hydrogen production.[11–13] Therefore, the lower theoretical potential (0.36 V) of the urea oxidation reaction (UOR) is chosen to replace OER and non-toxic and non-polluting gases N_2 and CO_2 are produced in UOR, the reaction equation as follows:[14]

$$\text{UOR: } CO(NH_2)_2 + 6OH^- \rightarrow N_2 + 5H_2O + CO_2 + 6e \quad (1)$$

$$\text{HER: } 6H_2O + 6e^- \rightarrow 3H_2 + 6OH^- \quad (2)$$

$$\text{Overall reaction: } CO(NH_2)_2 + H_2O \rightarrow N_2 + 3H_2 + CO_2 \quad (3)$$

At the same time, water pollution caused by urine has become one of the most serious environmental problems.[15–18] Urine mainly contains urea, which can be naturally converted into ammonia and nitrogen compounds, causing pollution to the atmospheric environment.[19–21] The pollution issues by electrolysis of urea wastewater can be significantly improved.[22–24] Thus, urea electrolysis has recently become the focus of attention.[25–27] It not only can treat wastewater but also contributes to high efficient hydrogen production.

Furthermore, highly active catalysts to increase the efficiency of hydrogen evolution is required. Although UOR can be effectively catalyzed by the precious metals,

*For correspondence

Electronic supplementary material: The online version of this article (https://doi.org/10.1007/s12039-019-1678-6) contains supplementary material, which is available to authorized users.

Published online: 19 October 2019

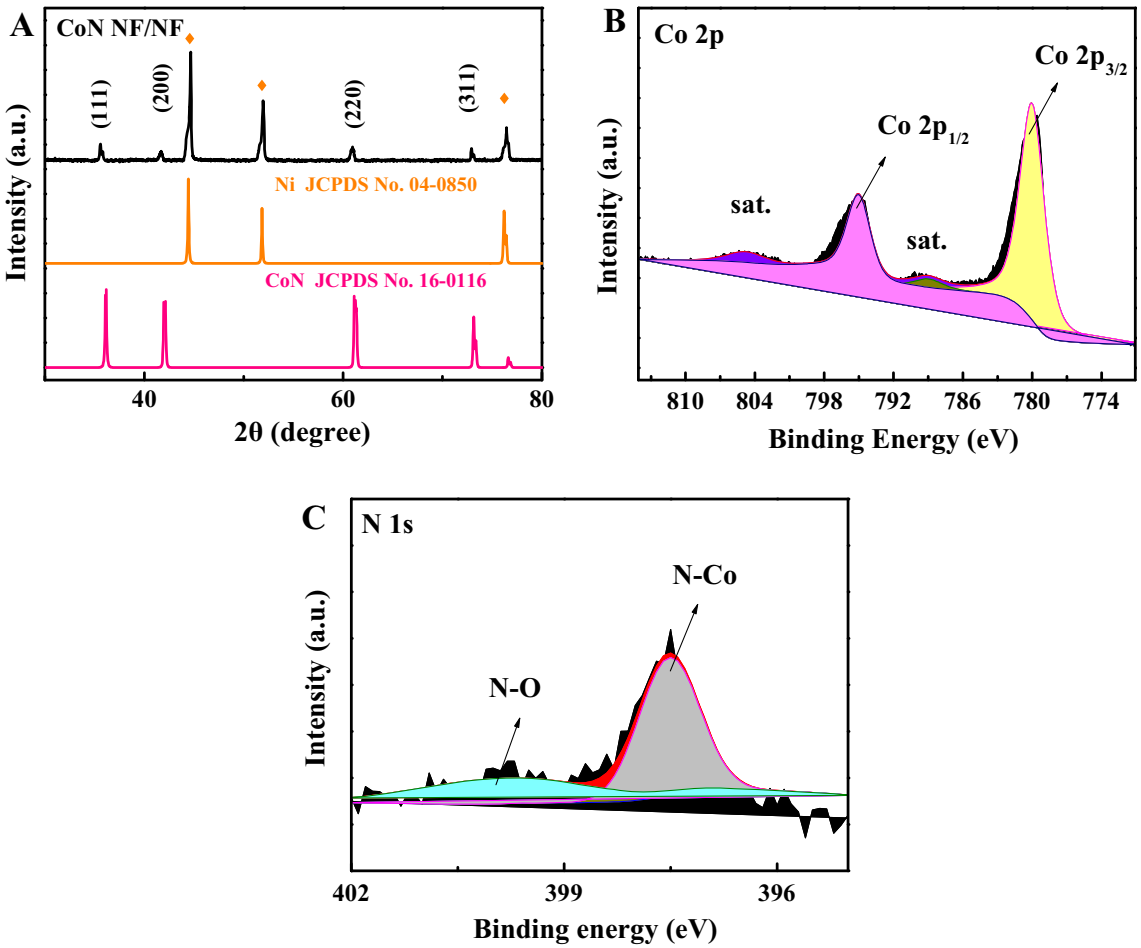

Figure 1. (A) XRD of CoN NF/NF. XPS of Co 2p (B), N 1 s (C) for CoN NF/NF.

such as Pt or Rh.[28,29] But their high cost makes it important to explore some low-cost and high-performance non-precious metal materials. More recently, various nitride materials, such as titanium nitride[30] and molybdenum nitride[31] have been proposed to be used in energy conversion and storage devices. Among them, particular interests are focused on CoN, which has fast charge transfer due to the electron delocalization modulation.[32] In this work, the CoN nanoflakes on Ni foam (CoN NF/NF) was prepared. The first process was the synthesis of CoO nanoflakes on Ni foam (CoO NF/NF) through a hydrothermal method. The second process was the synthesis of CoN NF/NF. The as-prepared CoO NF/NF above was placed in a ceramic crucible by a calcination method.

2. Experimental

2.1 *Materials*

Cobalt(II) chloride hexahydrate ($CoCl_2{\cdot}6H_2O$), Potassium hydroxide (KOH), urea, and hexamethylenetetramine were all purchased from Sinopharm Chemical Reagent Co. Ltd. (www.sinoreagent.com). 20 wt% Pt/C and 20 wt% IrO_2 were purchased from Shanxi Kaida Chemical Co. Ltd. (www.kd-chem.com). Nickel foam (NF) was purchased from Shenzhen Green and Creative Environmental Science and Technology Co. Ltd. All chemicals were used as received without further purification.

2.2 *Synthesis of CoN nanoflakes on Ni foam (CoN NF/NF)*

The first step was the synthesis of CoO nanoflakes on Ni foam (CoO NF/NF). 3 mmol $CoCl_2{\cdot}6H_2O$ and 10 mmol hexamethylenetetramine were dissolved in 25 mL ultra-pure water under constant stirring. After that, the suspension and pretreated Ni foam were transferred to a 50 mL Teflon-lined autoclave and heated at 100 °C for 10 h. The second step was the synthesis of CoN NF/NF. As the as-prepared CoO NF/NF above was placed in a ceramic crucible and calcined at 320 °C for 2 h (1 °C min^{-1}) under NH_3 flow.

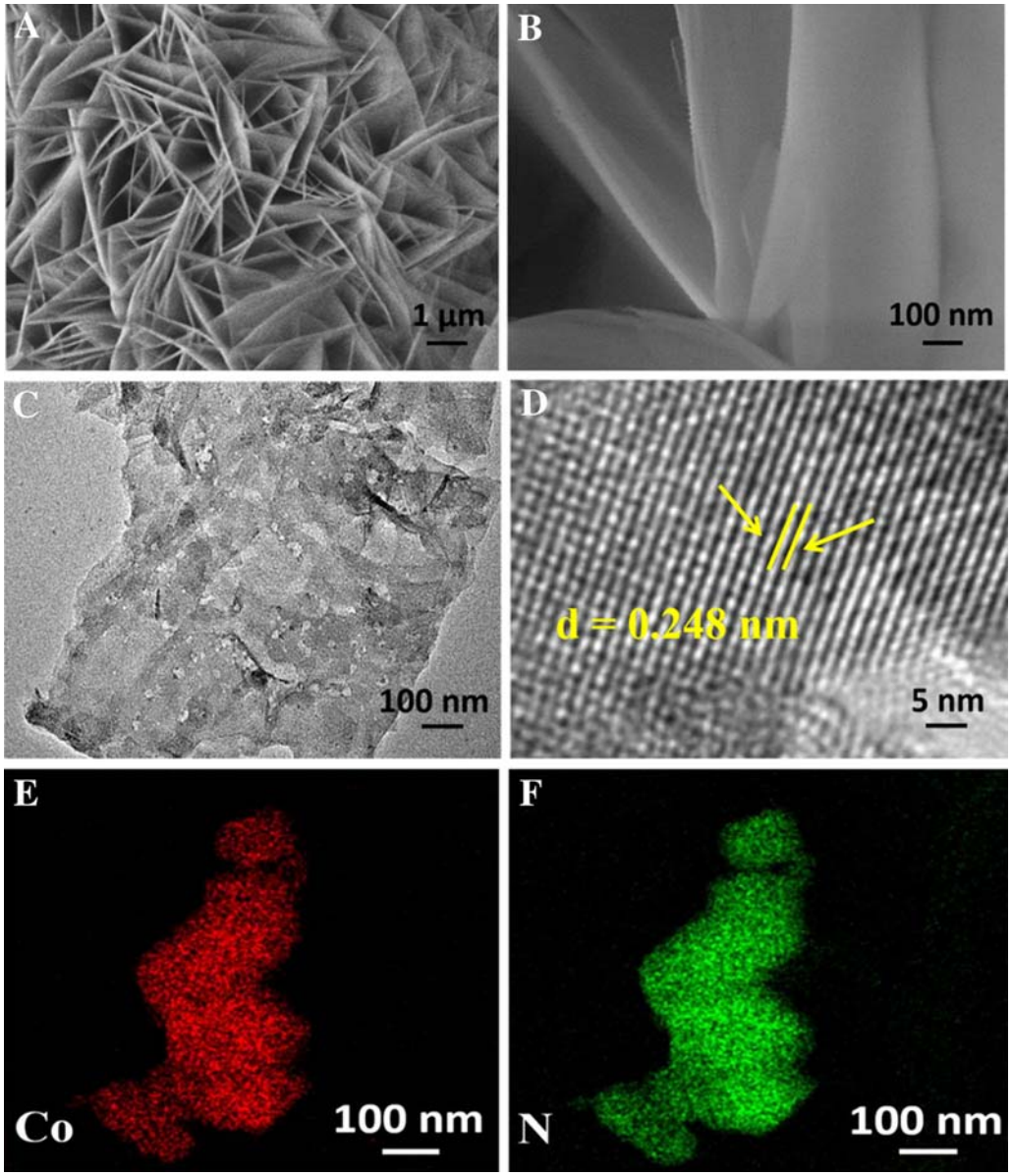

Figure 2. (A, B) SEM of CoN NF/NF. (C) TEM of CoN NF/NF. (D) HRTEM of CoN NF/NF. (E, F) Element mapping of CoN NF/NF.

2.3 *Physical characterization and electrochemical measurements*

XRD data were acquired on a RigakuD/MAX 2550 diffractometer with Cu Kα radiation (λ = 1.5418 Å). XPS measurements were performed on an ESCALABMK II X-ray photoelectron spectrometer using Mg as the exciting source. SEM measurements were carried out on an XL30 ESEM FEG scanning electron microscope at an accelerating voltage of 20 kV. TEM measurements were performed on a HITACHI H-8100 electron microscopy (Hitachi, Tokyo, Japan) with an accelerating voltage of 200 kV.

Electrochemical measurements were conducted on a CHI 660E electrochemical workstation with a standard three-electrode system. The prepared electrode materials were directly used as the working electrodes. The reference electrode was HgO/Hg (MOE) and the counter electrode was graphite rod. All of the measured potentials were converted to a reversible hydrogen electrode (RHE) according to the Nernst equation ($E_{RHE} = E_{Hg/HgO} + 0.098 + 0.059$ pH). The electrolyte is 1 M KOH with 0.5 M Urea. The electrochemical tests were measured at a scan rate of 5 mV/s under IR compensation. The electrochemical impedance spectroscopy (EIS) was conducted from frequency (Hz) 1 to 1000000.

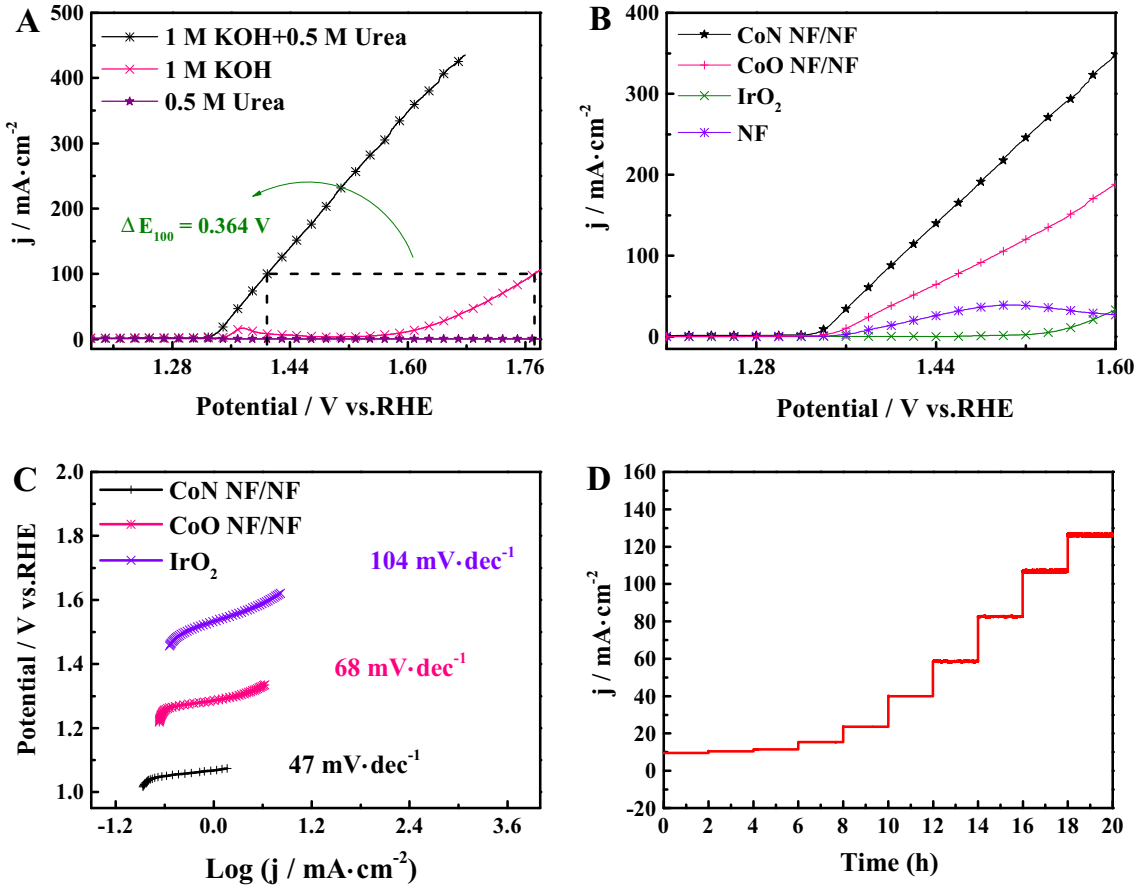

Figure 3. (A) LSVs of CoN NF/NF in different electrolytes. (B) LSVs and (C) Tafel slopes of CoN NF/NF, CoO NF/NF, IrO_2 and NF. (D) Multi-voltage process of CoN NF/NF.

3. Results and Discussion

3.1 *Physical characterization*

The XRD pattern of CoN NF/NF was shown in Figure 1(A). The diffraction peaks at 36.19°, 42.19°, 61.34°, and 73.32° corresponded to (111), (200), (220) and (311) crystal planes of CoN (JCPDS No. 16-0116), respectively. In addition, the peaks of 44.46°, 51.77° and 76.58° have a good correspondence with Ni (JCPDS No. 04-0850). While high-temperature calcination is used due to the introduction of nitrogen in the synthesis process, this may cause the material to have residual stress leading to a slight shift in the diffraction.[33,34] The results show that CoN NF/NF was successfully synthesized. CoO NF/NF also has a good match with standard cards (Figure S1, Supplementary Information). To further confirm the surface chemical composition of the prepared catalysts, Figure 1(B) shows the XPS spectrum of Co 2p for CoN NF/NF. The peak at 779.0 eV is consistent with Co $2p_{3/2}$, while the peak at 796.5 eV can correspond to Co $2p_{1/2}$.[35] Figure 1(C) reveals the XPS spectrum of N 1 s for CoN NF/NF, the peaks at 397.5 eV and 399.9 eV can be associated to N-Co and N-O.[36,37] Meanwhile, the chemical composition of CoN was measured in Table S1, Supplementary Information. The C, N, and Co atom % were 50.26, 23.83 and 25.91% respectively.

The morphologies of the as-prepared catalysts were observed by SEM. The SEM images of CoN NF/NF show that the Ni foam (Figure S2(A), Supplementary Information) is uniformly grown with CoN NF/NF nanoflakes (Figure 2(A)). It is clear that the CoN NF/NF is a fluffy and uniform layer structure (Figure 2(B)). CoO NF/NF also presents a sheet appearance (Figure S2(B), Supplementary Information). This indicates that CoN NF/NF nanoflakes with well-preserved morphology are successfully prepared after nitridation treatment. Figure 2(C) shows the TEM of CoN NF/NF. The sheet structure was clearly observed. As shown in Figure 2(D), the high-resolution transmission electron microscopy (HRTEM) of CoN NF/NF shows crystal stripes. Additionally, the inter lattice distances of 0.248 nm correspond to the CoN (111). This phenomenon is consistent with the conclusion obtained by XRD. The elemental mappings demonstrate that the Co (Figure 2(E)) and N (Figure 2(F)) elements are

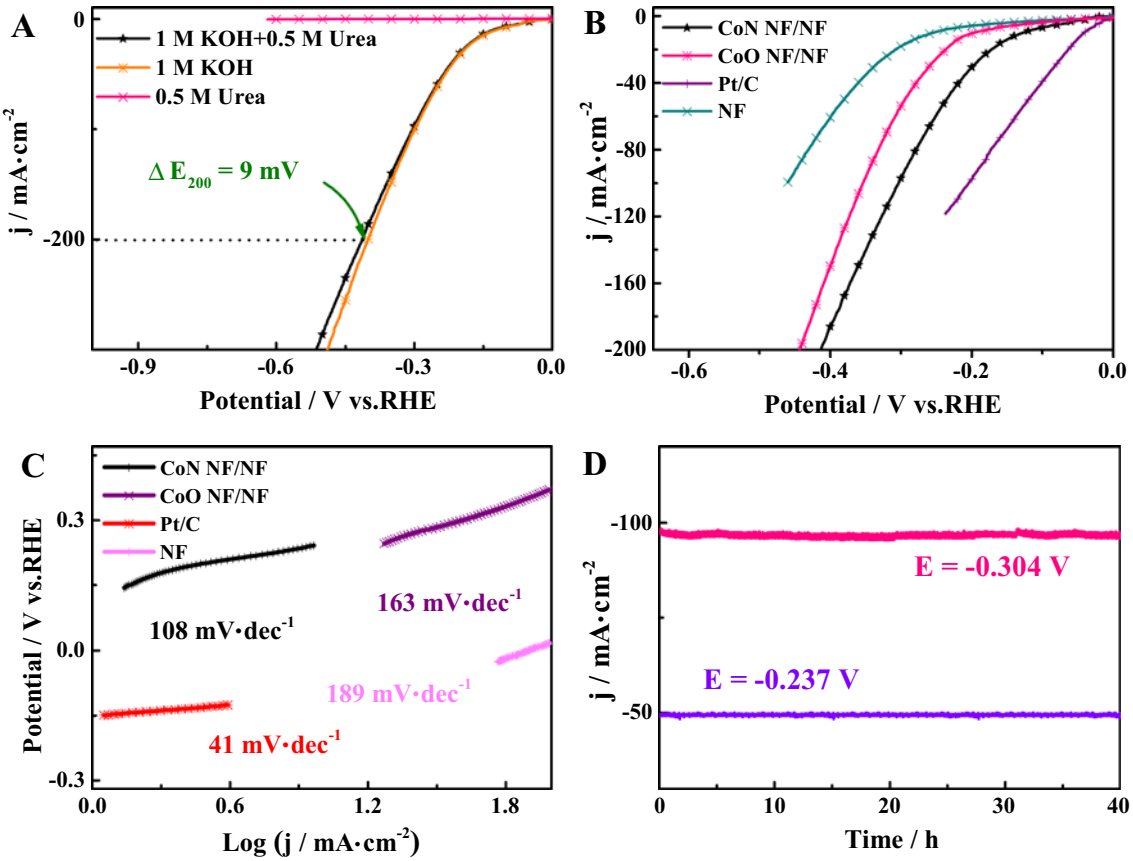

Figure 4. (A) LSVs of CoN NF/NF in different electrolytes. (B) LSVs and (C) Tafel slopes of CoN NF/NF, CoO NF/NF, IrO_2 and NF. (D) Chronoamperometry testing (i–t) of CoN NF/NF.

uniformly distributed throughout the layer structure, confirming the successful fabrication of cobalt nitride nanoflakes on NF. All these observations support the formation of CoN nanoflakes on NF.

3.2 *Electrochemical characterization*

The catalytic UOR activities of CoN NF/NF (loading: 0.82 mg/cm^2) were measured by electrochemical experiments and the most suitable urea concentration (0.5 M) was selected by the polarization curve of the concentration gradient (Figure S3, Supplementary Information). LSVs of CoN NF/NF was tested in different electrolytes as shown in Figure 3(A). At 100 mA/cm^2, UOR electrode potential is 1.409 V, which is 0.364 V lower than that of OER, which means UOR activity is better than that of OER. At 10 mA/cm^2, the potentials of CoN NF/NF, CoO NF/NF, IrO_2 and NF are 1.342, 1.362, 1.558 and 1.641 V, respectively as shown in Figure 3(B). Obviously, the potential of CoN NF/NF is the lowest. This phenomenon can be considered as UOR activities of CoN NF/NF better than that of others. The Tafel slopes of LSVs can be used to measure the electrode dynamics of the UOR.[38] The Tafel slopes for CoN NF/NF, CoO NF/NF, and IrO_2 are 47, 68, and 104 mV/dec, respectively (Figure 3(C)). It is obvious that the Tafel slope of CoN NF/NF is the lowest, reflecting its fast kinetics and excellent UOR catalytic activity.[39] Moreover, stability is vital to UOR. Figure 3(D) shows the multi-step chronopotentiometric curve of CoN NF/NF. Specifically, a staircase potential is applied to CoN NF/NF electrode from 1.35 V up to 1.43 V with an increment of 8 mV per 2 h. At the current starting value, the potential immediately levels off and remains constant for the remaining 2 h, especially at higher current. The fast chronopotentiometric response implies excellent mass transport. These results indicate that CoN NF/NF has excellent mass transportation, conductivity, and mechanical robustness (inward diffusion of OH and outwards diffusion of bubbles and fast response to current density in each potential change step).[40,41] This measurement lasts for 20 h and after 3000 CV cycles, it was observed that the current density can maintain 93.1% of the initial value (Figure S4, Supplementary Information). Meanwhile, the peaks from XRD are almost the same as those before

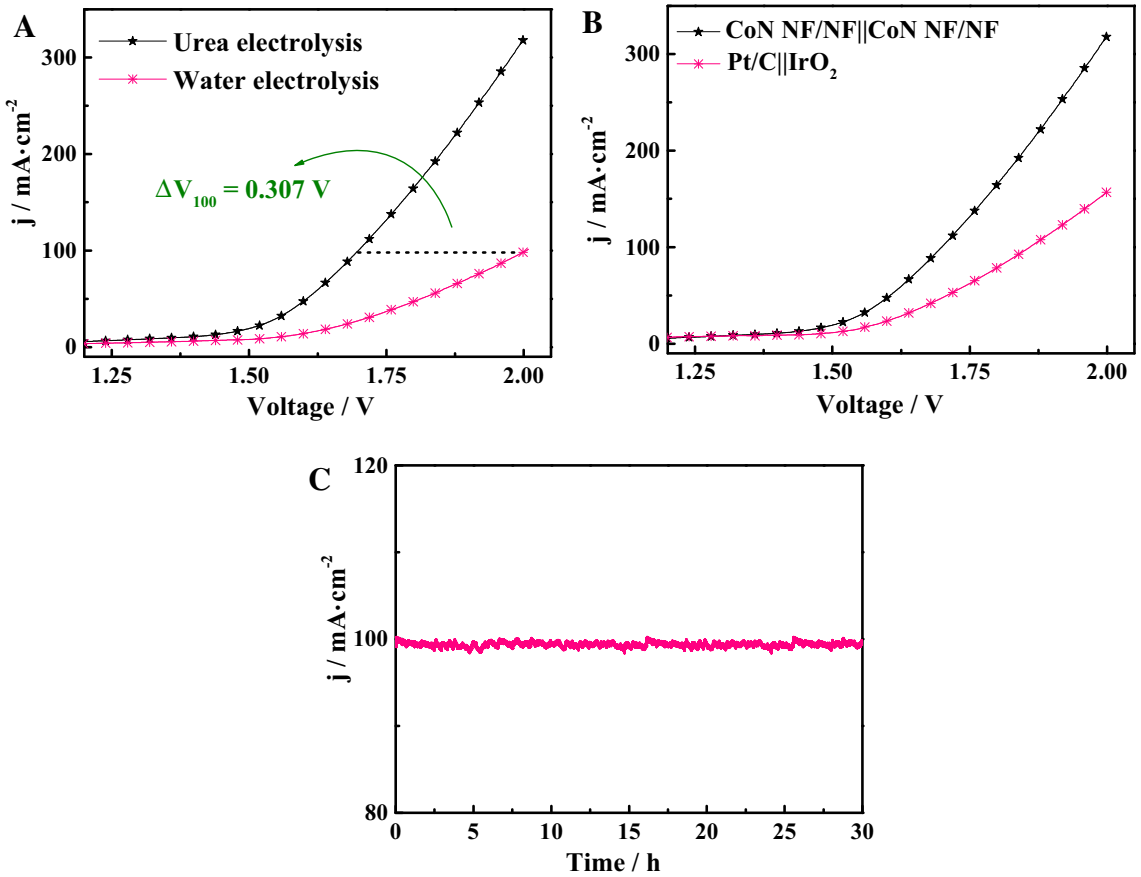

Figure 5. (A) LSVs of urea electrolysis and water electrolysis. (B) LSVs of CoN NF/NF||CoN NF/NF and Pt/C||IrO_2. (C) Chronoamperometric response of CoN NF/NF||CoN NF/NF.

3000 CV cycles, matches well with the standard cards (Figure S5, Supplementary Information). Those indicate the remarkable stability.[25]

To analyze the catalytic activities for HER, LSVs of CoN NF/NF was tested in different electrolytes (Figure 4(A)). The potential between electrolytes with and without urea at 200 mA/cm^2 (ΔE_{200}) is 9 mV. They have little difference, which indicates that urea has an insignificant effect on HER in KOH. Figure 4(B) shows the LSVs of the as-prepared catalysts. At 10 mA/cm^2, the potentials of CoN NF/NF, CoO NF/NF, Pt/C and NF are 129, 198, 42 and 256 mV, respectively. Although the overpotential of CoN NF/NF is higher than that of Pt/C, it is lower than that of CoO NF/NF and the impedance also shows the same conclusion (Figure S6, Supplementary Information). The Tafel slopes of CoN NF/NF, CoO NF/NF, Pt/C and NF are 108, 163, 41 and 189 mV/dec (Figure 4(C)). Obviously, the Tafel slope of CoN NF/NF is the closest to Pt/C, indicating it performs efficiently for HER. As shown in Figure 4(D), chronoamperometry testing (i–t) of CoN NF/NF at −0.304 and −0.237 V were performed. It shows that it can be stable for at least 40 h.

To explore the electrochemical properties of the CoN NF/NF electrode in overall urea oxidation, we performed a two-electrode electrolyzer using CoN NF/NF as anode and cathode (CoN NF/NF||CoN NF/NF). And IrO_2 as cathode and Pt/C as anode (Pt/C||IrO_2) are used to compare. Figure 5(A) represents LSVs of CoN NF/NF||CoN NF/NF. The voltage of urea electrolysis is 1.698 V, which is much lower than that of water electrolysis (2.005 V) at 100 mA/cm^2. This result demonstrates that urea electrolysis provides a significantly enhanced electrochemical performance when compared to water electrolysis. As shown in Figure 5(B), CoN NF/NF||CoN NF/NF needs voltages of 1.506 and 1.605 V at 20 and 50 mA/cm^2. While Pt/C||IrO_2 needs much higher value of 1.580 and 1.708 V. This result demonstrates that the performance of CoN NF/NF||CoN NF/NF electrolyzer is much higher than that of Pt/C||IrO_2. Meanwhile, the electrochemical properties of the materials in the literature were compared. The results show that CoN has better catalytic activity than others (Figure S7 and Table S2, Supplementary Information). Furthermore, chronoamperometry (i–t) measurement performed at an applied voltage of 1.7 V on urea electrolysis shows that CoN NF/NF||CoN NF/NF can sustain

a high current density over 30 h of operation (Figure 5(C)), demonstrating its high stability.

4. Conclusions

In summary, a simple and low-cost method is used to synthesize non-noble CoN nanoflakes catalyst supported on nickel foam (CoN NF/NF) for efficient urea electrolysis to produce hydrogen energy. When this catalyst CoN NF/NF is used as both the anode and cathode materials in a urea electrolyser, it exhibits excellent catalytic activity and long-term stability towards both HER and UOR. The potential of CoN NF/NF is 1.342 V at 10 mA/cm^2 on UOR. Such CoN NF/NF also exhibits high activity toward HER, which only needs 129 mV to achieve 10 mA/cm^2. Those enable CoN NF/NF to be a bifunctional electrocatalytic material for UOR and HER. The corresponding two-electrode electrolyzer (CoN NF/NF||CoN NF/NF) can drive 20 mA/cm^2 at 1.506 V, which are 0.145 V and 0.074 V less than that of water electrolysis and Pt/C||IrO_2. This result shows a promising alternative to precious metals used in electrolytic hydrogen production. CoN NF/NF||CoN NF/NF can maintain electrolysis for at least 20 h at 100 mA/cm^2, which implies it has excellent stability. Therefore, urea electrolysis is more efficient than electrolysis of water and the high activity and stability of the bifunctional catalyst should have high potential to replace precious metals for hydrogen production and treatment of industrial wastewater containing urea. This study provides a new idea to produce hydrogen using transition metal nitride nanoarrays.

Supplementary Information (SI)

Additional physical characterization and electrochemical tests and comparison tables of catalytic performance with some catalysts in recent literature. Supplementary Information is available at www.ias.ac.in/chemsci.

Acknowledgements

This work was funded by the Environmental Catalysis Innovative Research Team of Zhengzhou Normal University (No. 702010).

References

1. Anantharaj S, Ede S R, Karthick K, Sam Sankar S, Sangeetha K, Karthik P E and Kundu S 2018 Precision and correctness in the evaluation of electrocatalytic water splitting: revisiting activity parameters with a critical assessment *Energ. Environ. Sci.* **11** 744
2. Mota F M, Choi C H and Boppella R 2019 Arising synergetic and antagonistic effects in the design of Ni- and Ru-based water splitting electrocatalysts *J. Mater. Chem. A* **7** 639
3. Ojha K, Banerjee S and Ganguli A K 2017 Facile charge transport in FeN_x/Mo_2N/CNT nanocomposites for efficient hydrogen evolution reactions *J. Chem. Sci.* **129** 989
4. Tilak B V, Ramamurthy A C and Conway B E 1986 High performance electrode materials for the hydrogen evolution reaction from alkaline media *Chem. Sci.* **97** 359
5. Manoharan R 1997 Electrochemical hydrogen evolution on solid oxides RuO_2, $Ru_{0.7}Rh_{0.3}O_2$, and IrO_2, from acidic water *Chem. Sci.* **109** 1
6. Yan X, Tian L, He M and Chen X 2015 Three-dimensional crystalline/amorphous Co/Co_3O_4 core/shell nanosheets as efficient electrocatalysts for the hydrogen evolution reaction *Nano. Lett.* **15** 6015
7. Xu K, Chen P, Li X, Tong Y, Ding H, Wu X, Chu W, Peng Z, Wu C and Xie Y 2015 Metallic nickel nitride nanosheets realizing enhanced electrochemical water oxidation *J. Am. Chem. Soc.* **137** 4119
8. Pulipaka S, Koushik A K S and Deepa M 2019 Enhanced photoelectrochemical activity of Co-doped β-In2S3 nanoflakes as photoanodes for water splitting *RSC Adv.* **9** 1335
9. Wang J, Cui W, Liu Q, Xing Z, Asiri A M and Sun X 2016 Recent progress in cobalt-based heterogeneous catalysts for electrochemical water splitting *Adv. Mater.* **28** 215
10. Xu W, Zhang H, Li G and Wu Z 2014 Nickel-cobalt bimetallic anode catalysts for direct urea fuel cell *Sci. Rep.* **4** 58
11. Hu S, Feng C, Wang S, Liu J, Wu H, Zhang L and Zhang J 2019 Ni_3N/NF as bifunctional catalysts for both hydrogen generation and urea decomposition *ACS Appl. Mater. Inter.* **11** 13168
12. Ma M, Qu F, Ji X, Liu D, Hao S, Du G, Asiri A M, Yao Y, Chen L and Sun X 2017 Bimetallic nickel-substituted cobalt-borate nanowire array: an earth-abundant water oxidation electrocatalyst with superior activity and durability at near neutral pH *Small* **13** 1700394
13. Gwak J, Choun M and Lee J 2016 Alkaline ammonia electrolysis on electrodeposited platinum for controllable hydrogen production *ChemSusChem* **9** 403
14. Chen S, Duan J, Vasileff A and Qiao S Z 2016 Size fractionation of two-dimensional sub-nanometer thin manganese dioxide crystals towards superior urea electrocatalytic conversion *Angew Chem. Int. Ed. Engl.* **55** 3804
15. Fei J B, Cui Y, Yan X H, Qi W, Yang Y, Wang K W and Li J B 2008 Controlled preparation of MnO_2 hierarchical hollow nanostructures and their application in water treatment *Adv. Mater.* **20** 452
16. Barakat N A M, Alajami M, Alhaj Y, Obaid M and Al-Meer S 2017 Enhanced onset potential NiMn-decorated activated carbon as effective and applicable anode in urea fuel cells *Catal. Commun.* **97** 1304
17. Ding R, Qi L, Jia M and Wang H 2014 Facile synthesis of mesoporous spinel NiCo2O4 nanostructures as highly efficient electrocatalysts for urea electro-oxidation *Nanoscale* **6** 1369

18. Tyagi M, Tomar M and Gupta V 2013 NiO nanoparticle-based urea biosensor *Biosens. Bioelectron.* **41** 110
19. Ji R Y, Chan D S, Jow J J and Wu M S 2013 Formation of open-ended nickel hydroxide nanotubes on three-dimensional nickel framework for enhanced urea electrolysis *Electrochem. Commun.* **29** 21
20. Wu M S, Ji R Y and Zheng Y R 2014 Nickel hydroxide electrode with a monolayer of nanocup arrays as an effective electrocatalyst for enhanced electrolysis of urea *Electrochim. Acta* **114** 194
21. Yue Z, Yao S, Li Y, Zhu W and Zhang W 2018 Surface engineering of hierarchical $Ni(OH)_2$ nanosheet@-nanowire configuration toward superior urea electrolysis *Electrochim. Acta* **268** 211
22. Wang L, Li M, Huang Z, Li Y, Qi S, Yi C and Yang B 2014 Toward high capacity and stable manganese-spinel electrode materials: A case study of Ti-substituted system *J. Power Sources* **264** 282
23. Yan X, Tian L and Chen X 2015 Crystalline/amorphous Ni/NiO core/shell nanosheets as highly active electrocatalysts for hydrogen evolution reaction *J. Power Sources* **300** 336
24. Liu Q, Xie L, Qu F, Liu Z and Du G 2017 Porous Ni_3N nanosheets array as a high-performance nonnoble-metal catalyst for urea-assisted electrochemical hydrogen production *Inorg. Chem. Front.* **2017** 1120
25. Chen T, Liu D, Lu W, Wang K, Du G, Asiri A M and Sun X 2016 Three-dimensional Ni\r 2\r P nanoarray: an efficient catalyst electrode for sensitive and selective nonenzymatic glucose sensing with high specificity *Anal. Chem.* **88** 7885
26. Wu M, Jao C, Chuang and Chen F 2017 Carbon-encapsulated nickel-iron nanoparticles supported on nickel foam as a catalyst electrode for urea electrolysis *Electrochim. Acta* **227** 210
27. Wang X, Wang J, Sun X, Wei S, Cui L, Yang W and Liu J 2017 Hierarchical coral-like NiMoS nanohybrids as highly efficient bifunctional electrocatalysts for overall urea electrolysis *Nano Res.* **11** 988
28. Chen S, Duan J, Vasileff A and Qiao S Z 2016 Size fractionation of two-dimensional sub-nanometer thin manganese dioxide crystals towards superior urea electrocatalytic conversion *Angew. Chem. Int. Ed.* **55** 3804
29. Miller A T, Hassler B L and Botte G G 2012 Rhodium electrodeposition on nickel electrodes used for urea electrolysis *J. Appl. Electrochem.* **42** 925
30. Li F, Ohnishi R, Yamada Y, Kubota J, Domen K, Yamada A and Zhou H 2013 Carbon supported TiN nanoparticles: an efficient bifunctional catalyst for nonaqueous $Li–O_2$ batteries *Chem. Commun.* **49** 1175
31. Dong S, Chen X, Zhang K, Gu L, Zhang L, Zhou X, Li L, Liu Z, Han P, Xu H, Yao J, Zhang C, Zhang X, Shang C, Cui G and Chen L 2011 Molybdenum nitride based hybrid cathode for rechargeable lithium–O_2 batteries *Chem. Commun.* **47** 11291
32. Kang J S, Kim J Y, Yoon J, Kim J, Yang J, Chung D Y and Sung Y E 2018 Room-temperature vapor deposition of cobalt nitride nanofilms for mesoscopic and perovskite solar cells *Adv. Energy Mater.* **8** 1703114
33. Gelfi M, Bontempi E, Roberti R, Armelao L and Depero L E 2004 Residual stress analysis of thin films and coatings through XRD^2 experiments *Thin Solid Films* **450** 143
34. Song X, Chardonnet S, Savini G, Zhang S Y, Vorster W J J and Korsunsky A M 2008 Experimental/Modelling Study of Residual Stress in Al/SiCp Bent Bars by Synchrotron XRD and Slitting Eigenstrain *Methods. Mater. Sci. Forum* **571** 277
35. Tong Y, Chen P, Zhou T, Xu K, Chu W, Wu C and Xie Y 2017 A bifunctional hybrid electrocatalyst for oxygen reduction and evolution: cobalt oxide nanoparticles strongly coupled to B, N-Decorated Graphene *Angew. Chem. Int. Ed.* **129** 7227
36. Liu T, Li M, Dong P, Zhang Y and Guo L 2018 Design and facile synthesis of mesoporous cobalt nitride nanosheets modified by pyrolytic carbon for the nonenzymatic glucose detection *Sens. Actuat. B: Chem.* **255** 1983
37. Gao D, Zhang J, Wang T, Xiao W and Tao K 2016 Metallic Ni_3N nanosheets with exposed active surface sites for efficient hydrogen evolution *J. Mater. Chem. A* **4** 17363
38. Xiao C, Li S, Zhang X and MacFarlane D R 2017 $MnO_2/MnCo_2O_4$/Ni heterostructure with quadruple hierarchy: a bifunctional electrode architecture for overall urea oxidation *J. Mater. Chem. A* **5** 7825
39. Chen S, Duan J, Ran J, Jaroniec M and Qiao S 2013 N-doped graphene film-confined nickel nanoparticles as a highly efficient three-dimensional oxygen evolution electrocatalyst *Energy Environ. Sci.* **6** 3693
40. Lu X and Zhao C 2015 Electrodeposition of hierarchically structured three-dimensional nickel–iron electrodes for efficient oxygen evolution at high current densities *Nat. Commun.* **6** 6616
41. Liu D, Liu T, Zhang L, Qu F, Du G, Asiri A M and Sun X 2017 High-performance urea electrolysis towards less energy-intensive electrochemical hydrogen production using a bifunctional catalyst electrode *J. Mater. Chem. A* **5** 3208